# Study of surface exfoliation induced by hydrogen implantation and annealing in GaSb (100) substrates

Ravi Pathak, U. Dadwal, A.K. Kapoor, M. Vallet, Alain Claverie, R. Singh

# Study of surface exfoliation induced by hydrogen implantation and annealing in GaSb (100) substrates

Ravi Pathak[1]*, U. Dadwal[2], A. K. Kapoor[1], Maxim Vallet[3], Alain Claverie[3] and R. Singh[1,2]

[1]*Department of Physics, Indian Institute of Technology Delhi, New Delhi 110016, India*

[2]*Nanoscale Research Facility (NRF), Indian Institute of Technology Delhi, New Delhi 110016, India*

[3]*CEMES-CNRS and Universite de Toulouse, 29 rue J. Marvig, 31055 Toulouse, France*

**Abstract**

We investigate the surface blistering/exfoliation in H-implanted GaSb (100) substrates. Samples were implanted by 50 keV hydrogen ions with fluence of $5 \times 10^{16}$ and $1 \times 10^{17}$ ions/cm$^2$ at room temperature. Post-implantation annealing studies were carried out up to 300 ºC to observe surface blistering. For the samples implanted with fluence $5 \times 10^{16}$ ions/cm$^2$, annealing showed no sign of surface blistering. However, post-implantation annealing at 200 ºC for 2 min resulted in surface blistering for the samples implanted with fluence $1 \times 10^{17}$ ions/cm$^2$. Exfoliation of the surface in the form of craters was observed for $1 \times 10^{17}$ ions/cm$^2$ implantation case which was quantified using various parameters. Interestingly, surface exfoliation over large area was observed for both fluences after post-implantation annealing. High resolution X-ray diffraction studies of the H-implanted samples showed the existence of damage-induced strain and its dependence on the hydrogen fluence. Microstructural investigations of the damage region have been carried out using cross-sectional transmission electron microscopy. The width of the damage region and the formation of microstructures were found to depend on the fluence of hydrogen ions which eventually guides the surface blistering/exfoliation.

*Keywords*: Hydrogen; Implantation; GaSb; Strain; Exfoliation

**E-mail address*: ravipathak51189@gmail.com

## Introduction

Hydrogen (H) implantation in semiconductor materials has various applications in the microelectronic industry. One such application is the passivation of defects and the fine tuning of their electrical properties [1]. Hydrogen implantation is also used in the ion-cut process to transfer thin crystalline layers from a H-implanted substrate onto another host material [2-4]. In principle, it could be used for the heterogeneous integration of compound III–V semiconductors on a silicon platform for opto-electronic applications [5,6]. In this context, gallium antimonide (GaSb) is interesting because many compound semiconductors whose bandgap lies between 0.3 and 1.58 eV can be easily matched on its crystalline lattice [7]. Such GaSb/$SiO_2$/Si based substrates would be perfect for fabricating high frequency devices, laser diodes and infrared detectors [8–10]. Up to now, most of such structures are grown on semi-insulating gallium arsenide (GaAs) substrates [11,12]. The large lattice mismatch of ~7% between GaSb and GaAs inevitably results in high dislocation densities at the GaSb/GaAs interface [11,12]. To overcome the lattice mismatch problem, several attempts have been made including the use of low temperature buffer layers [13,14]. The ion-cut process could be an alternative approach to solve the issue by directly transferring high quality GaSb layers with controlled thickness onto silicon wafers.

Today, the ion-cut process is being used to fabricate most of the silicon-on-insulator (SOI) wafers sold on the planet [2-4]. Thus, the mechanism leading to the fracture of the material is well understood in silicon [15-18]. Hydrogen ions are implanted with doses and energies so that the hydrogen concentration reaches a few percent at the projected range of the ions. The hydrogen ions induce damage in the crystal lattice, initially as vacancies and interstitials which recombine during and following implantation at room temperature until stable complexes are formed [16,18]. During post-implantation annealing, these complexes transform and precipitate in the form of nanometer-size platelets which further grow in size by Ostwald

ripening and finally coalesce to form highly hydrogen pressurized micrometer-size cracks parallel to the wafer surface [17,19]. If the implantation depth is not too large, the surface can elastically relax the stress exerted by the hydrogen pressure inside the cavities. This gives rise to the appearance of blisters on the surface [17]. If the surface cannot relax this stress, because of its too large amplitude or because the cavities are too deep below the surface, cracks propagate parallel to the surface, eventually lifting off the top surface and leaving craters on the surface [20]. This is called layer exfoliation. The possibility to form blisters and exfoliate the material is admitted to be a prerequisite condition for the successful application of the ion-cut process of some material [21,22]. Indeed, in this process a "handle" wafer is bonded onto the implanted surface before annealing. Acting as a stiffener, it prevents the implanted material to elastically relax the stress generated by the cavities and favors crack formation and propagation until fracture of the whole wafer occurs [3,4]. This is why most research aimed at investigating the possibility of transferring new materials using the ion-cut process starts with the study of blistering/exfoliation phenomena. This work focuses on the study of hydrogen implantation and annealing induced surface exfoliation for the GaSb single crystalline substrate.

The conditions required for the transfer of high quality GaSb layers using the ion-cut process have not been much explored so far. Hobart and Kub showed that thin films of GaSb could be transferred onto insulating substrates using H-implantation in combination with direct wafer bonding [23]. Subsequently, Zheng *et al*. also performed H implantation-induced blistering/splitting studies in GaSb. The implantation involved 150 keV $H^+$ ions at a fluence of $5.5 \times 10^{16}$ $cm^{-2}$ [24]. In our preliminary work, we reported on surface blistering and exfoliation over regions of few micrometers in diameter in H-implanted GaSb [25]. Post-implantation annealing temperature and duration of annealing was varied from 200 to 500 °C and 1 minute to 80 minutes, respectively. This resulted in surface blisters of sizes 10 –20 µm along with

exfoliation extended over tens of micrometer area [23-25]. However, large surface area exfoliation, which is one of the favorable requirements for layer transfer, has not been reported so far. Also, there is no report available in the literature on different characteristics of the GaSb implanted layers which determine the efficiency and quality of the process. Thus, in the present work, we report on the influence of the implanted fluence onto the strain, onto the nature of microstructural damage resulting from ion implantation and annealing and finally, on blistering/exfoliation phenomena in GaSb.

**Experimental**

2-inch in diameter *p*-type Si doped (100) GaSb wafers were purchased from Wafer World, Inc. USA. They were diced to quarter size samples and implanted with 50 keV hydrogen ions at fluences of $5 \times 10^{16}$ or $1 \times 10^{17}$ ions/cm$^2$. H-implantation was carried out at room temperature (RT) with a current density of 10 $\mu$A cm$^{-2}$. The sample surface normal was set ~7° off the hydrogen ion beam to minimize ion channeling [26]. Post-implantation annealing was carried out in air using a box type furnace in the 200-400 °C range and for times ranging from 1 to 30 min [24,25]. The surface topography of the samples was investigated using an optical microscope (Nikon ECLIPSE LV100D) in Nomarski contrast mode and an atomic force microscope (AFM) from Bruker (Dimension Icon) in contact mode. The physical dimensions of the blisters were measured using a stylus surface profilometer (KLA-Tencor). The depth profile of the implanted hydrogen ions was measured by secondary ion mass spectroscopy (SIMS) using a CAMECA IMS 4F. The strain in the as-implanted sample was measured using high resolution X-ray diffraction (HRXRD). For that, triple-axis diffraction (TAD) $2\theta/\omega$ was carried out around the (004) Bragg peak using a Philips X'Pert PRO diffractometer. Microstructural investigations were carried by cross-sectional transmission electron microscopy (XTEM) using an aberration-corrected FEI TECNAIF20, equipped with an FEG

source. Samples were prepared by focused ion beam (FIB) techniques using a FEI Helios Nanolab 600 dual-beam FIB and SEM.

**Results and discussion**

The implantation of hydrogen ions in semiconductors gives rise to various defects and damages the crystal lattice [27,28]. After post-implantation annealing, these defects rearrange themselves in such a way to cause blistering/exfoliation of the implanted semiconductor wafers. Thus, the study of these defects in the as-implanted state becomes important. To understand the effect of hydrogen implantation in GaSb, the current study has been divided into two parts; (i) as-implanted and (ii) post-implantation annealing study of hydrogen implanted GaSb.

**As-implanted study of hydrogen implanted GaSb**

Fig. 1 shows the depth-distribution of hydrogen obtained by SIMS in the sample implanted with $1 \times 10^{17}$ $H^+/cm^{-2}$. The maximum hydrogen concentration is $3.25 \times 10^{21}$ atom/$cm^3$ at a depth of ~ 410 nm from the sample surface. The area under the SIMS profile, which represents the fluence of hydrogen actually implanted within GaSb, was found to be approximately equal to the hydrogen fluence to which the material was submitted, indicating that there was no fluence loss of hydrogen ions during or after implantation. The energy of the H-implanted ions decides the projected range of ions inside the material. Fig. 2 shows the result of the Monte Carlo simulation of this implantation using the Stopping and Range of Ions in Matter (SRIM) code [29]. The simulation predicts about the same concentration of hydrogen but at a slightly larger depth (~ 440 nm) than measured by SIMS. The damage profile, which represents the distribution of point defects initially generated by the implant, has its maximum at a slightly shallower depth ( ~390 nm from the top of the H-implanted surface).

To investigate the hydrogen-induced damage in GaSb, cross-sectional TEM measurements of the two samples were carried out in the as-implanted state. Fig. 3 shows a set of cross-sectional TEM images of the sample implanted at a fluence of $5 \times 10^{16}$. Fig. 3a is a bright field image taken under dynamical diffraction conditions. Under such conditions, the black regions in the image denote the strain fields generated by the defects resulting from the implantation. A "damage band" containing these defects is found centered at a depth of about 420 nm from the top of the surface and extends over a width of about 115 nm. Fig. 3b is a high magnification image of the same sample but taken under out-of-Bragg, out-of-focus conditions, suitable for the detection of gas-filled objects through the Fresnel contrast they generate in the image [18]. This image shows alignments of nano-bubbles and the presence of platelets and nano-cracks, 50 to 80 nm in diameter, preferably at the bottom of the damage band (mean depth 460 nm), both aligned parallel to the surface. Fig. 4a is a bright field image of the sample implanted at $1 \times 10^{17}$ ions/cm$^2$. The damage band has substantially increased in width, now at about 190 nm, but is centered at a shallower depth than it was. In other words, when increasing the fluence, the damage band has extended more on its surface side than on its deep side. Fig. 4b shows that the damage band is filled with platelets and alignments of nano-bubbles. Numerous nano-cracks are visible, confined at the very bottom of the damage band. Some of them have visibly coalesced, forming larger cracks more or less parallel to the wafer surface. Still, the material is not fractured as there exist regions between the cracks which are not delaminated.

The implantation of hydrogen ions generates defect complexes that lead to the distortion or strain in the lattice (Modelling of point defect complex formation and its application to H+ ion implanted silicon, N. Cherkashin et al., Acta Materialia 99 (2015) 187–195). HRXRD investigations have been carried out to determine the effect of fluence on the strain and thereby on blistering or exfoliation in H-implanted GaSb. A TAD $2\theta/\omega$ scan was carried out around (004) Bragg peak. Fig. 5 shows the XRD profiles we have recorded on these samples around

**Commenté [c1]:** In silicon, it is demonstrated that strain is mostly generated by HnVm complexes. VH4 and V2V6 are the most efficient to generate strain.

their (004) Bragg peaks, normal to the wafer surfaces. For the pristine GaSb, a sharp peak is observed at the characteristic angle $\theta_B = 60.72^{o}$. For the implanted samples, this peak has shifted toward $\theta_B = 60.32^{o}$ and $60.24^{o}$, for the samples implanted at $5 \times 10^{16}$ and $1 \times 10^{17}$ ions/cm$^2$, respectively. These negative shifts demonstrate the deformation of the implanted layers, which increases with the fluence. Reboh. *et al*. [30] and more recently, Cherkashin et al. have discussed in detail this behaviour in H-implanted silicon [31]. Following implantation, numerous defect complexes are formed. Their overall effect is to put the implanted layer under compression. As in pseudomorphic heterostructures, this stress cannot relax in-plane and the material thus reacts by generating an out-of-plane (perpendicular to the wafer surface) tensile strain, $\varepsilon_z = \left(\frac{\Delta d}{d}\right)_z$, where $d$ is the interplanar spacing between (004) planes and $\Delta d$ is the change in this interplanar spacing due to H-induced damage. From the experimentally observed shifts of the Bragg's peaks, we find $\varepsilon_z \sim 0.65$ % and ~ 0.79 % for the samples implanted with $5 \times 10^{16}$ and $1 \times 10^{17}$ H$^+$/cm$^2$, respectively. Assuming the material is isotropic, the in-plane compressive stresses at the origin of these strains can be calculated from the relation, $\sigma_{xx} = -2\mu\left(\frac{\Delta d}{d}\right)_z$, where μ is the shear modulus of the material [30]. Taking μ = 24.1 GPa for GaSb, we get in-plane compressive stresses of $-482$ and $-578$ MPa for the two respective fluence values. Moreover, the full width at half maximum (FWHM) of the damage peak, which is an indication of the width of the damage region, also increases with the fluence, from 0.042 to 0.065 and is in agreement with the TEM observations.

**Post-implantation annealing study of hydrogen implanted GaSb**

Surface blistering is a complex phenomenon and is required to observe layer splitting in H-implanted semiconductors. H-induced blistering depends on various implantation parameters such as ion fluence and implantation temperature [32-34]. Post-implantation annealing

parameters *viz* temperature and time also affect the surface blistering [25,34]. Thus, both these post-implantation parameters have been varied to study the surface blistering of GaSb samples. Fig. 6a and 6b show optical images of the surfaces of the GaSb samples implanted with $5 \times 10^{16}$ $H^+/cm^{-2}$ after annealing at 200 ºC for 2 and 5 min, respectively. Though annealing was expected to result in surface blistering however, we observed large area surface exfoliation as can be seen in fig 6a. Increasing the annealing time to 5 min finally resulted in the total exfoliation of the implanted layer. Fig. 7a, 7b, 7c and 7d show the optical images of the GaSb samples implanted with $1 \times 10^{17}$ $cm^{-2}$ after isothermal annealing at 200 ºC for 2, 5, 10 and 30 min, respectively. After 2 min annealing, blisters are seen on the surface with diameters and heights in the 2 to 10 μm and 30 to 90 nm ranges, respectively, as measured by profilometry (Fig. 7a). Moreover, in a few places, craters are also observed with sizes ranging from 10 to 50 μm. These craters are thought to result from the exfoliation of the material due to the coalescence of a group of blisters. When increasing the annealing time, the craters get distributed uniformly over the surface while their density increases (Fig. 7*b*, 7*c* and 7*d*)), visibly at the expense of the surface region.

Fig. 8a is an AFM image obtained in contact mode of the edge of a surface crater (see red circle in Fig. 7a). Fig. 8b is a line-scan extracted from this image. This scan shows that the edge of the crater is somehow curved upward and that the distance between the top edge and the bottom of the crater is of about ~ 474 nm. This compares well with the depth at which the nanocracks have been detected by XTEM in the as implanted sample (see Fig. 4b).

Alternatively, Fig. 9a, 9b, 9c and 9d show the optical images of the GaSb samples after 10 min isochronal annealing at 200, 225, 250 and 300 ºC, respectively. These figures show that the percentage of the surface which is exfoliated increases with the annealing temperature. Thus, exfoliation behavior of the H-implanted GaSb was assessed as a function of annealing temperature. To quantify this aspect, we have defined three characteristic parameters: (*i*)

exfoliation efficiency ($A_{ex}$); defined as $A_{ex}(\%) = A_{ex}^{total}/A_{image}^{total} \times 100$, where $A_{ex}^{total}$ is the total exfoliation area obtained by sum of the individual exfoliated areas and $A_{image}^{total}$ is the total area of the image, (*ii*) mean exfoliation area ($S_{ex}$); defined as $S_{ex} = A_{ex}^{total}/N_{ex}$, where $N_{ex}$ is the total number of the individual exfoliation areas measured in the image, and (*iii*) exfoliation density ($D_{ex}$); defined as $D_{ex} = N_{ex}/A_{image}^{total}$ [35]. These parameters were calculated from the images obtained from the Nomarski optical microscopy and the corresponding results are given in Table 1. For each annealing temperature, different regions of the exfoliated areas were selected to calculated these parameters.

Table. 1. Exfoliation efficiency $A_{ex}$, mean exfoliation area $S_{ex}$ and the exfoliation density $D_{ex}$ for the GaSb samples implanted with 50 keV hydrogen ions for a fluence of $1 \times 10^{17}$ cm$^{-2}$ at room temperature. The samples were annealed at 200, 225, 250 and 300 ºC for 10 min, respectively.

| **Annealing Temperature (ºC)** | $A_{ex}$ | $S_{ex}$ ($\mu m^2$) | $D_{ex}$ |
|---|---|---|---|
| 200 | 42% | 5.25 | 0.076 |
| 225 | 52% | 6.10 | 0.082 |
| 250 | 58% | 8.75 | 0.069 |
| 300 | 100% | NA | NA |

It was found out that with the increase in the annealing temperature, the exfoliation efficiency $A_{ex}$ and the mean exfoliation area $S_{ex}$ increased (see Table 1). However, the exfoliation density $D_{ex}$ first increases and reaches a value of 0.082 for 225 ºC and then decreases. This could be due to the implanted hydrogen which nucleates the implantation-induced cavities in the damage region. The increase in the exfoliation efficiency $A_{ex}$ and the mean exfoliation area $S_{ex}$ with the annealing temperature is related to the concentration of hydrogen atoms within these H-induced cavities inside the damage region. Reboh *et al*. reported that with the increase in the annealing temperature, the internal pressure within the cavities increases which results in the

coalescence of neighboring cavities [36]. When the pressure inside cavities is high enough, the exfoliation of the top surface occurs in the form of surface craters. However, for annealing at temperature 300 ºC, large area exfoliation of the top surface was observed (Fig. 9d). Also, the exfoliation of the top surface for the implantation with fluence $5 \times 10^{16}$ ions/cm$^2$ occurs at 200 ºC for 5 min. On the other hand, for the implantation with fluence $1 \times 10^{17}$ ions/cm$^2$, exfoliation was observed at a higher temperature of 300 ºC for 10 min. This could be due to the formation of the narrow damage band in the case of implantation with fluence $5 \times 10^{16}$ ions/cm$^2$. H-induced defects generated are distributed in a narrow damage region and upon post-implantation annealing, hydrogen is released from the H-induced defects complexes and accumulates inside the extended defects (platelets). Consequently, platelets grow to form nanocracks and eventually lead to the formation of large cracks parallel to the H-implanted surface which resulted in surface exfoliation after post-implantation annealing at a lower temperature.

## Conclusion

In conclusion, we have investigated the blistering/exfoliation in the H-implanted GaSb as a function of ions fluence. Samples implanted with fluence of $5 \times 10^{16}$ ions/cm$^2$ showed exfoliation of the top surface after post-implantation annealing at 200 ºC for 5 min. However, for the samples implanted with fluence $1 \times 10^{17}$ ions/cm$^2$, exfoliation of the surface along with craters was observed after post-implantation annealing at 300 ºC for 10 min. The exfoliation behavior of the H-implanted samples with annealing temperature was investigated using three parameters: exfoliation efficiency, mean exfoliation area and exfoliation density. It was observed that the exfoliation efficiency and mean exfoliation area increase with the increase in annealing temperature. HRXRD showed the dependence of H-induced strain on the fluence of implanted ions. Damage-induced strain was found to be more in the case of implantation with fluence $1 \times 10^{17}$ ions/cm$^2$. Microstructural investigation revealed the formation of damage region decorated with extended defects in the form of platelets of size between 50 and 80 nm for fluence $5 \times 10^{16}$ ions/cm$^2$ and nanocracks formation for fluence $1 \times 10^{17}$ ions/cm$^2$. The width of the damage region was found to be less in the case of H-implantation for the fluence $5 \times 10^{16}$ ions/cm$^2$. This resulted in narrow distribution of the defects within the damage region resulting blistering after post-implantation annealing and eventually exfoliation of the top surface.

## Acknowledgments

The authors would like to acknowledge the Nanoscale Research Facility (NRF), Indian Institute of Technology Delhi, New Delhi for supporting this work.

**References**


1. J. Pankove, N. Johnson, Hydrogen in semiconductors, Semiconductors and Semimetals, Vol. 34, Academic Press, 1991.
2. M. Bruel, Silicon on insulator material technology, Electon. Lett. 31 (1995) 1201-1202.
3. Q-Y Tong, U.M. Gösele, Wafer Bonding and Layer Splitting for Microsystems, Adv. Mater. 11 (1999) 1409-1425.
4. S.H. Christiansen, R. Singh, U. Gösele, Wafer Direct Bonding: From Advanced Substrate Engineering to Future Applications in Micro/Nanoelectronics , Proc. IEEE 94 (2006) 2060-2106.
5. R. Singh, I. Radu, R. Scholz, C. Himcinschi, U. Gösele, S.H. Christiansen, Investigation of helium implantation induced blistering in InP, J. Lumin. 121 (2006) 379-382.
6. U. Dadwal, A. Kumar, R. Scholz, M. Reiche, P. Kumar, G. Boehm, M.C. Amann, R. Singh, Blistering study of H-implanted InGaAs for potential heterointegration applications, Semicond. Sci. Technol. 26 (2011) 085032.
7. P.S. Dutta, H.L. Bhat, V. Kumar, The physics and technology of gallium antimonide: An emerging optoelectronic material, J. Appl. Phys. 81 (1997) 5821.
8. K. Akahane, N. Yamamoto, S.I. Gozu, N. Ohtani, Heteroepitaxial growth of GaSb on Si(0 0 1) substrates, J. Cryst. Growth 264 (2004) 21-25.
9. E.H. Aifer, J.G. Tischler, J.H. Warner, I. Vurgaftman, W.W. Bewley, J.R. Meyer, J.C. Kim, L.J. Whitman, C.L. Canedy, E.M. Jackson, W-structured type-II superlattice long-wave infrared photodiodes with high quantum efficiency, Appl. Phys. Lett. 89 (2006) 053519.
10. K.F. Longenbach, W.I. Wang, Molecular beam epitaxy of GaSb, Appl. Phys. Lett. 59 (1991) 2427.
11. B. Brar, D. Leonard, Spiral growth of GaSb on (001) GaAs using molecular beam epitaxy, Appl. Phys. Lett. 463 (1995) 463.

12. R.M. Graham, A.C. Jones, N.J. Mason, S. Rushworth, L. Smith, P.J. Walker, Growth of GaSb on GaAs substrates, J. Cryst. Growth 145 (1994) 363-370.
13. S.V. Ivanov, P.D. Altukhov, T.S. Argunova, A.A. Bakun, A.A. Budza, V.V. Chaldyshev, A. Yu Kovalenko, P.S. Kop'ev, R.N. Kutt, B. Ya Meltser, S.S. Ruvimov, S.V. Shaposhnikov, L.M. Sorokin, V.M. Ustinov, Molecular beam epitaxy growth and characterization of thin (<2 mu m) GaSb layers on GaAs (100) substrates, Semicond. Sci. Technol. 8 (1993) 347.
14. E.T.R. Chidley, S.K. Haywood, A.B. Henriques, N.J. Mason, R.J. Nicholas, P.J. Walker, Photoluminescence of GaSb grown by metal-organic vapour phase epitaxy, Semicond. Sci. Technol. 6 (1991) 45.
15. T. Höchbauer, A. Misra, M. Nastasi, J.W. Mayer, Physical mechanisms behind the ion-cut in hydrogen implanted silicon, J. Appl. Phys. 92 (2002) 2335.
16. M. Nastasi, T. Höchbauer, J.K. Lee, A. Misra, J.P. Hirth, M. Ridgway. T. Lafford, Nucleation and growth of platelets in hydrogen-ion-implanted silicon, Appl. Phys. Lett. 86 (2005) 154102.
17. L-J Huang, Q-Y Tong, Y-L Chao, T-H Lee, T. Martini, U. Gösele, Onset of blistering in hydrogen-implanted silicon, Appl. Phys. Lett. 74 (1999) 982.
18. J. Grisolia, G. Ben Assayag, A. Claverie, B. Aspar, C. Lagahe, L. Laanab, A transmission electron microscopy quantitative study of the growth kinetics of H platelets in Si, Appl. Phys. Lett. 76 (2000) 852.
19. M.K. Weldon, V.E. Marsico, Y.J. Chabal, A. Agarwal, D.J Eaglesham, J. Sapjeta, W.L. Brown, D.C. Jacobson, Y. Caudano, S.B. Christman, E.E. Chaban, On the mechanism of the hydrogen-induced exfoliation of silicon, J. Vac. Sci. Technol. B 15 (1997) 1065.
20. S. Reboh, A.A. De Mattos, J.F. Barbot, A. Declemy, M.F. Beaufort, R.M. Papaĺo, C.P. Bergmann, P.F.P. Fichtner, Localized exfoliation versus delamination in H and He

coimplanted (001) Si, J. Appl. Phys. 105 (2009) 093528.

21. J.K. Lee, M. Nastasi, N.D. Theodore, A. Smalley, T.L. Alford, J.W. Mayer, M. Cai, S.S. Lau, Effects of hydrogen implantation temperature on ion-cut of silicon, J. Appl. Phys. 96 (2004) 280.
22. O. Moutanabbir, A. Giguère, B. Terreault, Narrow fluence window and giant isotope effect in low-energy hydrogen ion blistering of silicon, Appl. Phys. Lett. 84 (2004) 3286.
23. K.D. Hobart and F.J. Kub, Transfer of GaSb thin film to insulating substrate via separation by hydrogen implantation, Electron. Lett. 35 (1999) 675.
24. Y. Zheng, P.D. Moran, Z.F. Guan, S.S. Lau, D.M. Hansen, T.F. Kuech, T.E. Haynes, T. Hoechbauer, M. Nastasi, Transfer of n-type GaSb onto GaAs substrate by hydrogen implantation and wafer bonding, J. Electron. Mater. 29 (2000) 916-920.
25. R. Pathak, U. Dadwal, R. Singh, Study of hydrogen implantation-induced blistering in GaSb for potential layer transfer applications, J. Phys. D: Appl. Phys. 50 (2017) 285301.
26. J.D. Plummer, D.D. Michael, B.P. Griffin, Silicon VLSI Technology, Englewood Cliffs, NJ: Prentice-Hall, 2000.
27. N. Daghbouj, N. Cherkashin, F.-X. Darras, V. Paillard, M. Fnaiech, A. Claverie, Effect of the order of $He^+$ and $H^+$ ion co-implantation on damage generation and thermal evolution of complexes, platelets, and blisters in silicon, J. Appl. Phys. 119 (2016) 135308.
28. S. Personnic, K.K. Bourdelle, F. Letertre, A. Tauzin, N. Cherkashin, A. Claverie, R. Fortunier, H. Klocker, Impact of the transient formation of molecular hydrogen on the microcrack nucleation and evolution in H-implanted Si (001), J. Appl. Phys. 103 (2008) 023508.
29. J.F. Ziegler, J.P. Biersack, U. Littmark, The Stopping and ranges of Ions in Matter, Pergamon Press, New York, 1995.
30. S. Reboh, M.F. Beaufort, J.F. Barbot, J. Grilhé, P.F.P. Fichtner, Orientation of H platelets

under local stress in Si, Appl. Phy. Lett. 93 (2008) 022106.

31. N. Cherkashin, N. Daghbouj, G. Seine, A. Claverie, Impact of He and H relative depth distributions on the result of sequential $He^+$ and $H^+$ ion implantation and annealing in silicon, J. Appl. Phys. 2018, 123, 161556.
32. B.S. Li, Z.G. Wang, Y.Y. Du, K.F. Wei, C.F. Yao, M.H. Cui, Y.F. Li, H.P. Zhu, Effect of implantation temperature on exfoliation of $H_2^+$-implanted Si, Vacuum 109 (2014) 1-7.
33. O. Moutanabbir, B. Terreault, M. Chicoine, F. Schiettekatte, The fluence effect in hydrogen-ion cleaving of silicon at the sub-100-nm scale, Appl. Phys. A 80 (2005) 1455-1462.
34. U. Dadwal, P. Kumar, O. Moutanabbir, M. Reiche, R. Singh, Effect of implantation temperature on the H-induced microstructural damage in AlN, J. Alloys Compd. 588 (2014) 300-304.
35. H.J. Woo, H.W. Choi, G.D. Kim, J.K. Kim, K.J. Kim, Blistering/exfoliation kinetics of GaAs by hydrogen and helium implantations, Surf. Coat. Technol. 203 (2009) 2370-2374.
36. S. Reboh, J.F. Barbot, M.F. Beaufort, P.F.P. Fichtner, H-induced subcritical crack propagation and interaction phenomena in (001) Si using He-cracks templates, Appl. Phy. Lett. 96 (2010) 031907.

**Figure captions**

**Fig. 1** Experimental depth-distribution (SIMS profile) of hydogen after $1 \times 10^{17}$ $H^+/cm^2$, 50 keV ion implantation into GaSb.

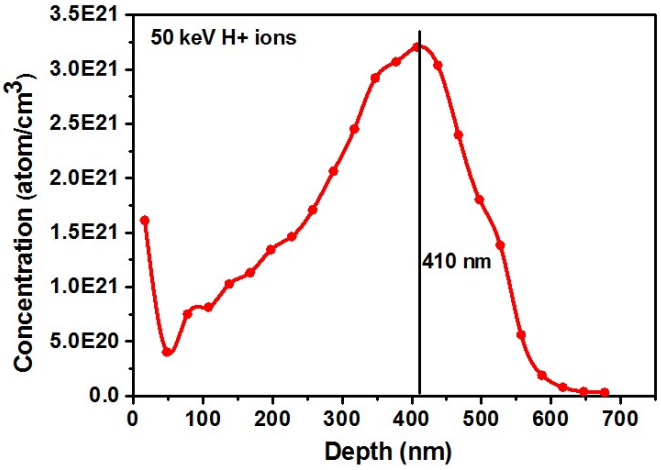


**Fig. 2** Monte Carlo simulations of the ion and damage profiles (SRIM code) resulting from 50 keV $H^+$ ions in GaSb sample.

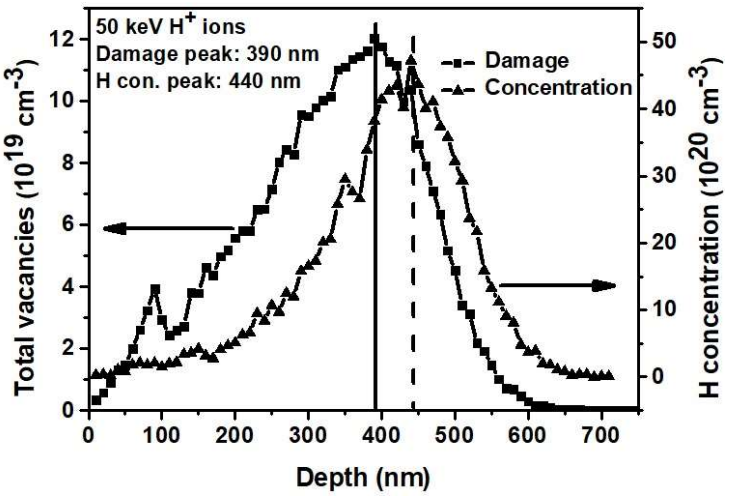


**Fig. 3** (a) Cross-sectional TEM image of the GaSb sample implanted with 50 keV $H^+$ ions with the fluence of $5 \times 10^{16}$ ions/cm$^2$. (b) high magnification cross-sectional TEM image of the damage region.

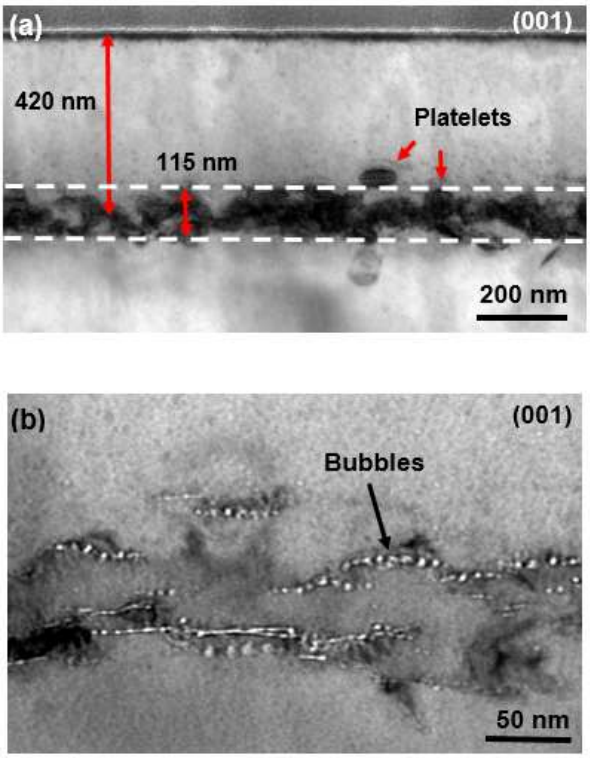


**Fig. 4** (a) Cross-sectional TEM image of GaSb sample implanted with 50 keV $H^+$ ions with the fluence of $1 \times 10^{17}$ ions/cm$^2$. (b) The high magnification cross-sectional TEM image of the damage region.

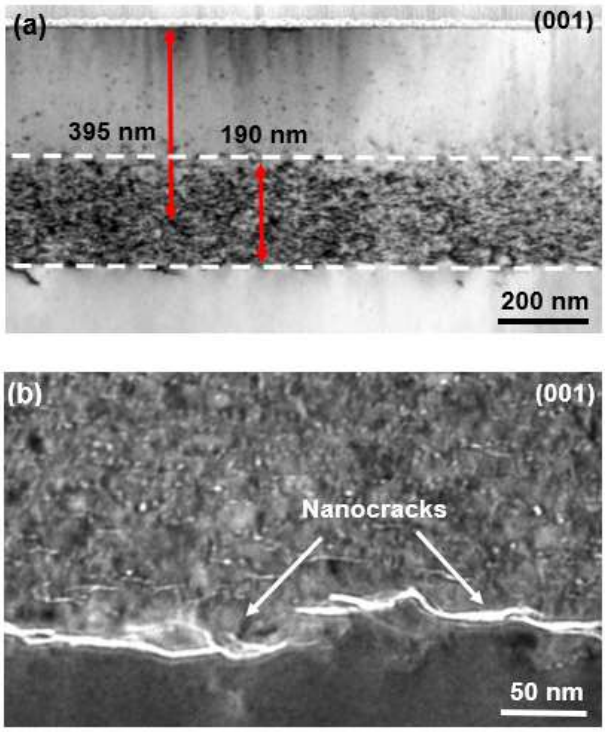


**Fig. 5** HRXRD of the pristine GaSb sample and the H-implanted samples with fluence 5 × $10^{16}$ ions/cm$^2$ and 1 × $10^{17}$ ions/cm$^2$, respectively. A triple-axis diffraction (TAD) $2\theta/\omega$ scan was carried out around (004) Bragg peak.

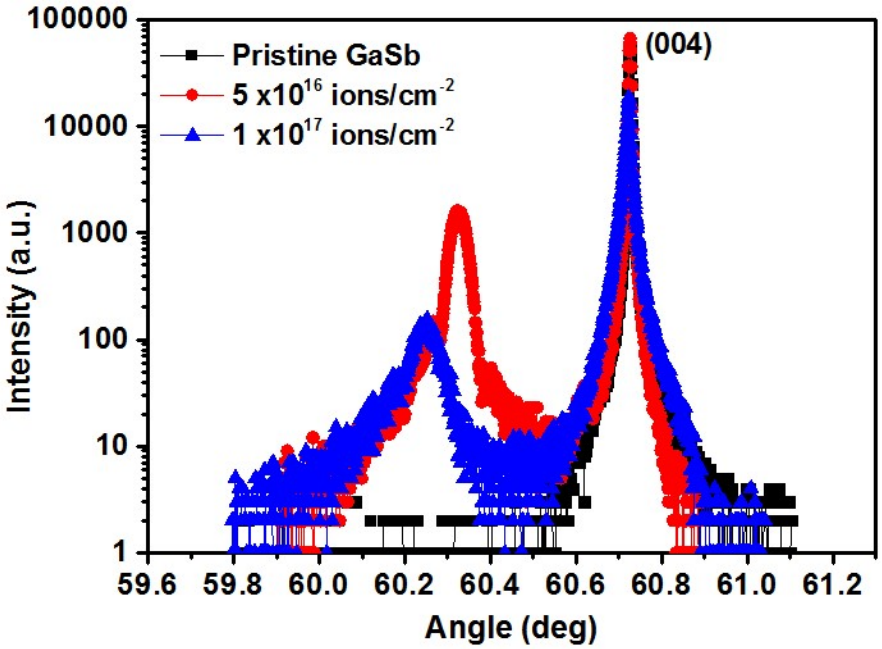


**Fig. 6** Nomarski optical images of the GaSb samples after post-implantation annealing at 200 ºC for (*a*) 2 min, and (*b*) 5 min. H-implantation was carried out at room temperature with ions fluence of $5 \times 10^{16}$ ions/cm$^2$.

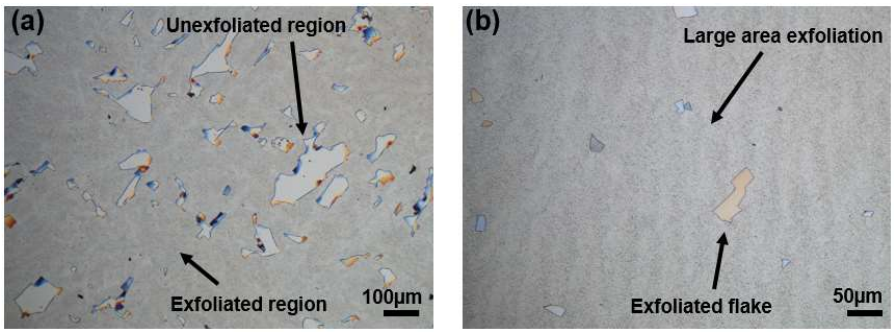
(a)
Unexfoliated region
Exfoliated region
100μm
(b)
Large area exfoliation
Exfoliated flake
50μm

**Fig. 7** Nomarski optical images of the GaSb samples after post-implantation annealing at 200 ºC for (*a*) 2 min, (*b*) 5 min, (*c*) 10 min, and (*d*) 30 min. H-implantation was carried out at room temperature with ions fluence of $1 \times 10^{17}$ ions/cm$^2$.

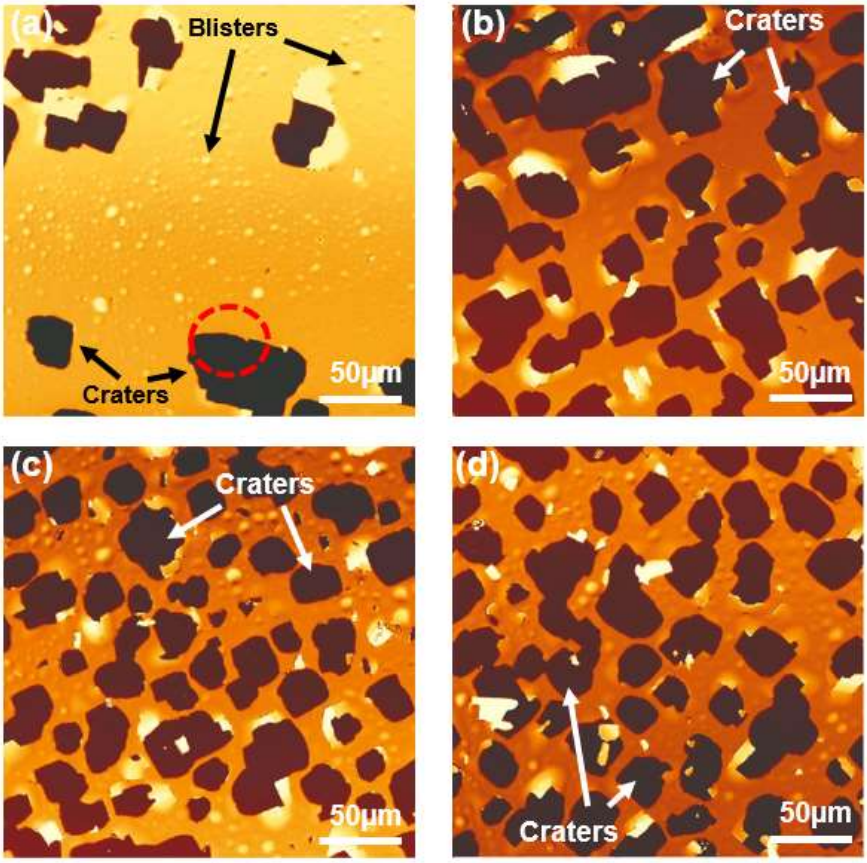

**Fig. 8** (*a*) AFM scan at the edge of the surface crater (see red circle in Fig. 7a). (*b*) AFM sectional measurement at the edge of the surface crater. H-implantation was carried out at room temperature with ions fluence of $1 \times 10^{17}$ ions/cm$^2$.

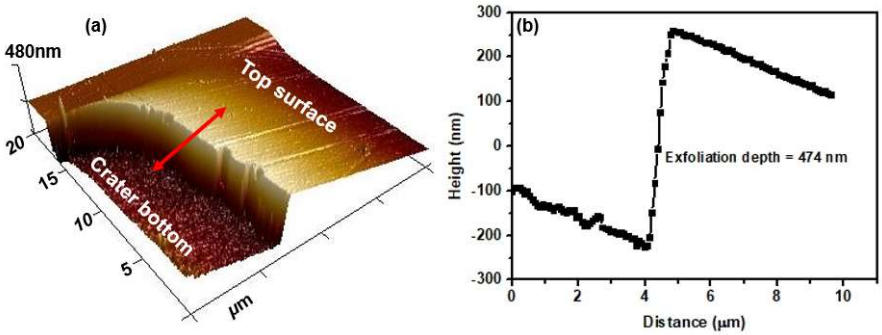

**Fig. 8** Nomarski optical images of the GaSb samples after the post-implantation annealing at (*a*) 200 ºC, (*b*) 225 ºC, (*c*) 250 ºC, and (*d*) 300 ºC. Post-implantation annealing studies were carried out for a fixed duration 10 min in all the cases. H-implantation was carried out at room temperature with ions fluence of $1 \times 10^{17}$ ions/cm$^2$.